

The N-Terminal Domain of Bcl-x_L Reversibly Binds Membranes in a pH-Dependent Manner[†]

Guruvasuthevan R. Thuduppathy,[‡] Oihana Terrones,[§] Jeffrey W. Craig,[‡] Gorka Basañez,[§] and R. Blake Hill^{*,‡,||}

Department of Biology, Johns Hopkins University, Baltimore, Maryland 21218, Unidad de Biofísica, Universidad del País Vasco, 48080 Bilbao, Spain, and Department of Chemistry, Johns Hopkins University, Baltimore, Maryland 21218

Received August 15, 2006; Revised Manuscript Received October 3, 2006

ABSTRACT: Bcl-x_L regulates apoptosis by maintaining the integrity of the mitochondrial outer membrane by adopting both soluble and membrane-associated forms. The membrane-associated conformation does not require a conserved, C-terminal transmembrane domain and appears to be inserted into the bilayer of synthetic membranes as assessed by membrane permeabilization and critical surface pressure measurements. Membrane association is reversible and is regulated by the cooperative binding of approximately two protons to the protein. Two acidic residues, Glu153 and Asp156, that lie in a conserved hairpin of Bcl-x_LΔTM appear to be important in this process on the basis of a 16% increase in the level of membrane association of the double mutant E153Q/D156N. Contrary to that for the wild type, membrane permeabilization for the mutant is not correlated with membrane association. Monolayer surface pressure measurements suggest that this effect is primarily due to less membrane penetration. These results suggest that E153 and D156 are important for the Bcl-x_LΔTM conformational change and that membrane binding can be distinct from membrane permeabilization. Taken together, these studies support a model in which Bcl-x_L activity is controlled by reversible insertion of its N-terminal domain into the mitochondrial outer membrane. Future studies with Bcl-x_L mutants such as E153Q/D156N should allow determination of the relative contributions of membrane binding, insertion, and permeabilization to the regulation of apoptosis.

Bcl-2 proteins act as checkpoints in the regulation of apoptosis by integrating intracellular signals to control the permeability and possibly the morphology of the mitochondrion (1–9). For many Bcl-2 proteins, this checkpoint involves a change in localization from the cytosol to the mitochondrion (10–13). For example, Bcl-x_L displays mixed localization to the cytosol and to organellar membranes, including the mitochondrion. After an apoptotic stimulus, Bcl-x_L appears to localize primarily to the mitochondrial outer membrane where it may bind other apoptotic factors such as Bad (10, 11, 14) or form an ion channel thought to maintain the integrity of the mitochondrial membrane (11, 15–17). While mixed localization of Bcl-x_L is well-established, the relative importance of cytosolic- and membranous-localized protein to the regulation of apoptosis is not. Intriguingly, the membrane activity of Bcl-x_L may

contribute more to its anti-apoptotic activity than its ability to sequester pro-apoptotic proteins: a mutant of Bcl-x_L with altered ion conductance properties (the XB mutant) decreased the anti-apoptotic activity of Bcl-x_L to a greater extent than a mutant unable to bind BH3 proteins such as Bax (15).

The ion conductance properties of Bcl-x_L most likely arise from a membrane conformation much different than the known solution conformation. It is difficult to envision how a soluble helical bundle (Figure 5a) would conduct ions, even though it is anchored into the mitochondrial outer membrane by a C-terminal transmembrane domain (TM).¹ One possibility is that this transmembrane domain self-assembles to mediate ion conductance. However, a construct lacking the transmembrane domain, Bcl-x_LΔTM, retains ion conductance properties similar to those of the full-length molecule if the pH of the solution is lowered (16). Thus, Bcl-x_L ion conductance likely involves a structural rearrangement to a membrane conformation of its soluble N-terminal domain and does not require its transmembrane domain.

Bcl-x_LΔTM indeed undergoes a conformational change in the presence of acidic lipids and at acidic pH (18–20).

[†] This work was supported by National Institutes of Health (NIH) Grant RO1GM067180 (to R.B.H.), American Cancer Society Award IRG-58-005-41 (to R.B.H.), and Ministerio de Ciencia y Tecnología Grant BFU2005-06095 (to G.B.). NMR instrumentation was secured in part from awards from the National Science Foundation (DBI-0216077) and NIH (S10-RR020922). G.R.T. was supported in part by the Dimitri V. d'Arbeloff award from the Millipore Foundation. O.T. was a recipient of a predoctoral fellowship from the Basque Government. J.W.C. was supported in part by HHMI and Pfizer summer undergraduate research fellowships.

* To whom correspondence should be addressed: Department of Biology, Mudd Hall, Johns Hopkins University, 3400 N. Charles St., Baltimore, MD 21218. Phone: (410) 516-6783. Fax: (702) 441-2490. E-mail: hill@jhu.edu.

[‡] Department of Biology, Johns Hopkins University.

[§] Universidad del País Vasco.

^{||} Department of Chemistry, Johns Hopkins University.

¹ Abbreviations: TM, transmembrane domain; LUV, large unilamellar vesicles; DOPC, 1,2-dioleoyl-*sn*-glycero-3-phosphocholine; DOPG, 1,2-dioleoyl-*sn*-glycero-3-[phospho-*rac*-(1-glycerol)]; DOPE, 1,2-dioleoyl-*sn*-glycero-3-phosphoethanolamine; ANTS, 8-aminonaphthalene-1,3,6-trisulfonate; DPX, *p*-xylene bis(pyridinium bromide); HEPES, 4-(2-hydroxyethyl)-1-piperazineethanesulfonic acid; Tris, tris(hydroxymethyl)aminomethane; DTT, dithiothreitol; GdnHCl, guanidinium hydrochloride; HSQC, heteronuclear single-quantum coherence; NOE, nuclear Overhauser enhancement.

While the structure of this membrane conformation is not known, it is helical (19, 21, 22) but without defined tertiary structure as measured by the lack of long-range NOEs (21) and near-UV circular dichroism spectropolarimetry (19). However, the inherent difficulties in charactering a protein with such structural polymorphism leave open many questions about the nature of this membrane conformation and how it is formed.

Here we present experiments designed to further characterize this conformational change. Because full-length Bcl-x_L is anchored to the membrane by its transmembrane domain, experiments with this construct are not ideal for understanding the conformational change that primarily involves the N-terminal domain. Therefore, in this work, we describe experiments with synthetic lipid vesicles and Bcl-x_LΔTM, a construct that retains pro-survival activity in vivo (23). We determine the pH dependence of this process by testing for protein association with lipid vesicles as a function of pH with a sedimentation assay. The nature of the conformational change is pursued using monolayer surface pressure and vesicle permeabilization experiments. Finally, we evaluate a mutant for altered conformational change properties to test whether conserved acidic residues in the hydrophobic helical hairpin affect this process. Surprisingly, we find that this conformational change is reversible and is described fairly well by a simplified thermodynamic linkage model involving the binding of approximately two protons. These results suggest that Bcl-x_L activity could be regulated by reversible membrane insertion of its N-terminal domain.

MATERIALS AND METHODS

Mutagenesis, Protein Expression, and Purification. Site-directed mutagenesis was carried out on the wild-type sequence of Bcl-x_LΔTM using the Quikchange mutagenesis kit (Stratagene) using standard procedures (24). The mutant and the wild-type plasmids were transformed into *Escherichia coli* Tuner DE3 (Stratagene) cells for overexpression. The constructs, the wild-type Bcl-x_LΔTM sequence, and the mutants all lack the C-terminal hydrophobic segment (residues 210–233). The purification of the wild-type protein has been described previously, and the mutant proteins were isolated in a similar manner (19). The purity of the final preparation was judged to be >95% as evaluated by Coomassie-stained SDS–PAGE. The proteins were stored at 4 °C in TEND buffer [20 mM Tris (pH 8.0) containing 1 mM EDTA, 500 mM NaCl, and 1 mM DTT] until further use. The mutant protein was shown to be monomeric by size exclusion chromatography and natively folded by circular dichroism spectropolarimetry (data not shown).

Lipid Vesicle Sedimentation Assay. Binding of protein to lipid vesicles was assessed using a sedimentation assay as previously described (19). This assay uses brominated lipids and allows for sedimentation using a tabletop microfuge and avoids nonidealities introduced at higher centrifugal forces using nonbrominated lipids (25). Large unilamellar vesicles were made by extrusion as described previously (26) with a lipid composition of DOPC and DOPG (60:40) doped with 0.25% lissamine rhodamine B-labeled DOPE added to visualize the lipid fraction. For binding experiments, 10 μM protein was incubated with 2.5 mM lipid vesicles (P:L, 1:250) overnight at 25 °C as a function of pH using Perrin's

constant-ionic strength (*I* = 0.05) buffers (27). NaCl was added to a final concentration of 150 mM to give a final ionic strength of 0.2 M.

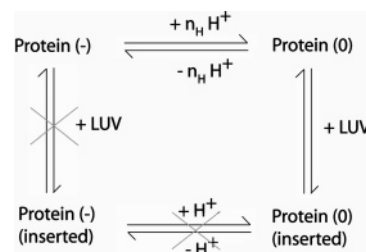
To determine the *K*_x for protein–lipid binding, the concentration of the protein in the supernatant after centrifugation was determined by the Bradford assay (28). A standard curve for the Bradford assay was generated from known concentrations of Bcl-x_LΔTM, determined by the absorbance at 280 nm in the presence of 6 M GdnHCl using a calculated extinction coefficient of 41 810 M^{−1} cm^{−1}. The amount of Bcl-x_LΔTM bound to the vesicles was estimated using the difference between the amount of protein used in the reaction and the amount of protein remaining in the supernatant. The percentage of protein bound to the vesicles was calculated as follows:

$$\% \text{ protein bound} = \left(1 - \frac{[P]_{\text{free}}}{[P]_{\text{total}}}\right) \times 100 \quad (1)$$

To test for reversibility, Bcl-x_LΔTM was incubated with lipid vesicles at pH 4.0 overnight. The sample was then split into two equal parts, one that was maintained at pH 4.0 and another that was titrated to pH 7.0 with the addition of small amounts of 0.1 N NaOH. Both the samples were then subjected to centrifugation after which the supernatant was removed and assayed for total protein using the Bradford assay.

Surface Pressure Measurements. Surface pressure measurements were carried out with a MicroTrough-S system from Kibron (Helsinki, Finland) at 37 °C with constant stirring. The lipid, dissolved in chloroform and methanol (2:1), was gently spread over the surface and kept at a constant surface area. The desired initial surface pressure, π_i , was attained by changing the amount of lipid applied to the air–water interface. After 10 min to allow for solvent evaporation, the protein was injected through a hole connected to the subphase. The final protein concentration in the Langmuir trough was 0.75 μM. The change in surface pressure, $\Delta\pi$, was recorded as a function of time until a stable signal was obtained. The subphase buffer was 1.0 mL of 150 mM KCl buffered with MES and KOH (pH 7.0) or potassium acetate and acetic acid (pH 5.0). The linear plot of $\Delta\pi$ as a function of π_i can be extrapolated to a $\Delta\pi$ of 0 to give the critical pressure, π_c , which is a measure of the relative “penetration capacity” of a protein into the monolayer (29–31).

Thermodynamic Model. A simple thermodynamic model was developed to describe the solution to the membrane conformational change of Bcl-x_LΔTM. This model couples the protonation equilibrium of the protein with the attractive partitioning equilibrium into the membrane:



and leads to the development of a coupled equilibria from which the fraction of protein bound (*F*_{bound}) to lipid vesicles

is determined by the following relationships:

$$\text{pH} = \text{p}K_a + \log \frac{[\text{P}_{\text{deprot}}]}{[\text{P}_{\text{prot}}]} \quad (2)$$

$$[\text{P}_{\text{total}}] = [\text{P}_{\text{deprot}}] + [\text{P}_{\text{prot}}] + [\text{P}_{\text{bound}}] \quad (3)$$

$$K_x = \frac{\frac{[\text{P}_{\text{bound}}]}{[\text{L}]}}{\frac{[\text{P}_{\text{prot}}]}{[\text{W}]}} \quad (4)$$

For n_H protons

$$\log \frac{[\text{P}_{\text{deprot}}]}{[\text{P}_{\text{prot}}]} = n_H(\text{pH} - \text{p}K_a) \quad (5)$$

$$\frac{[\text{P}_{\text{deprot}}]}{[\text{P}_{\text{prot}}]} = 10^{n_H(\text{pH} - \text{p}K_a)} \quad (6)$$

$$F_{\text{bound}} = \frac{[\text{P}_{\text{bound}}]}{[\text{P}_{\text{total}}]} = \frac{1}{1 + \frac{[\text{W}][1 + 10^{n_H(\text{pH} - \text{p}K_a)}]}{K_x[\text{L}]}} \quad (7)$$

where P_{deprot} is the protein that is completely deprotonated at the critical residues, the protonation of which defines the pH profile of binding, P_{prot} is the completely protonated version of the protein, P_{bound} corresponds to the population of the protein that is bound to the lipid vesicles, and $[\text{L}]$ and $[\text{W}]$ refer to the lipid and water concentrations, respectively. The parameters that are estimated by the fitting process are n_H , $\text{p}K_a^{\text{app}}$, and K_x . n_H is the number of protons that defines the pH profile. $\text{p}K_a^{\text{app}}$ is a measure of the protonation–deprotonation equilibrium involving those protons. K_x is the partition coefficient for the protonated Bcl-x_LΔTM to partition into the lipid vesicles. This framework has four assumptions: (i) only protonated Bcl-x_LΔTM [protein(0) above] binds to the lipid vesicles, (ii) membrane-bound protein is not involved in the protonation–deprotonation equilibrium, (iii) the protonation sites are equal and independent, and (iv) no significant contribution arises from the protonation–deprotonation equilibria of the ionizable lipid headgroups in this pH range (3–8). This last assumption is well-founded (32).

Lipid Vesicle Leakage Assay. DOPC and DOPG (60:40) lipids were mixed in organic solvent, evaporated thoroughly, and resuspended in 12.5 mM 8-aminonaphthalene-1,3,6-trisulfonate (ANTS), 45 mM *p*-xylene bis(pyridinium bromide) (DPX), 20 mM KCl, and 10 mM HEPES (pH 7.0). LUVs were prepared as described above, and nonencapsulated fluorescent probes were separated from the vesicle suspension through a Sephadex G-10 column loaded with 100 mM KCl and 10 mM Hepes (pH 7.0). Solution osmolarities were routinely checked with an Osmomat 030 instrument (Gonotec, Berlin, Germany). The size of the final LUV preparation was close to the expected value (100 nm) as determined by quasi-elastic light scattering using a Coulter N4 plus particle size analyzer. The phospholipid concentration was measured using the method of Bartlett (33). The leakage of encapsulated solutes was assayed as described

by Ellens et al. (34). The ANTS/DPX-loaded lipid vesicles (final lipid concentration of 0.1 mM) were treated with the appropriate amounts of Bcl-x_LΔTM or its mutants in a fluorimeter cuvette at 37 °C with constant stirring. Changes in fluorescence intensity were recorded in a Perkin-Elmer Life Sciences LS-50 spectrofluorometer with excitation and emission wavelengths set at 350 and 510 nm, respectively. An interference filter with a nominal cutoff value of 470 nm was placed in the emission light path to minimize the contribution of the light scattered by the vesicles to the fluorescence signal. The percentage of leakage was calculated after the complete release of the fluorescent probe by the addition of Triton X-100 [final concentration of 0.1% (w/v)].

NMR Spectroscopy. ¹⁵N-labeled Bcl-x_LΔTM was prepared as described previously (19). The protein (60 μM) in 20 mM sodium phosphate (pH 7.25) was incubated with lipid vesicles (60:40 DOPC:DOPG ratio) overnight at room temperature. The lipid concentration was 12 mM, resulting in a protein:lipid (P:L) ratio of 1:200. ¹H–¹⁵N HSQC experiments were carried out on a Bruker AVANCE 600 MHz spectrometer equipped with a cryoprobe; 1278 × 200 points were collected with sweep widths of 10 000 and 1520 Hz in ¹H and ¹⁵N, respectively, with the ¹⁵N carrier frequency set at 119.5 ppm. Sixteen transients were averaged for each *t*₁ point. The sample was titrated to pH 4.65 by the addition of small amounts of 0.1 N HCl. A HSQC spectrum was collected at this pH, and then the sample was titrated to pH 7.4 by the addition of small amounts of 0.1 N NaOH. Another HSQC spectrum was collected at this pH. All data were processed using NMRPipe and analyzed using NMRView (35–37).

RESULTS

Membrane Association of Bcl-x_LΔTM Appears To Be Reversible. We previously reported that the N-terminal domain of Bcl-x_L does not appreciably associate with lipid vesicles near physiological pH but does so completely at pH 4.9 in the absence of NaCl (18, 19). Here we tested for the reversibility of this membrane association in a vesicle sedimentation assay. In this assay, protein and lipid vesicles are incubated and then physically separated by centrifugation. For Bcl-x_LΔTM at pH 7.0 and 150 mM NaCl, we observe ~10% of the protein associated with lipid vesicles composed of DOPC and DOPG (60:40 and a 1:200 protein:lipid ratio), consistent with our earlier observations (19). When the pH of this sample was lowered to 4.0 via the addition of small amounts of concentrated HCl and resedimented, less than 5% of Bcl-x_LΔTM was detected in the supernatant, indicating nearly complete association with lipid vesicles (Figure 1). This membrane association involves a structural rearrangement and not protein precipitation that was demonstrated by changes in thermodynamic stability, tryptophan fluorescence, and circular dichroism spectroscopy (19). When this sample was returned to pH 7.0 via the addition of small amounts of concentrated NaOH, more than 92% of the protein returned to the supernatant, suggesting a near-complete reversal of membrane association.

Bcl-x_LΔTM that returns to solution after membrane association may be misfolded or unfolded, which cannot be detected in our sedimentation assay. Therefore, we repeated a similar titration experiment but monitored the ¹H and ¹⁵N

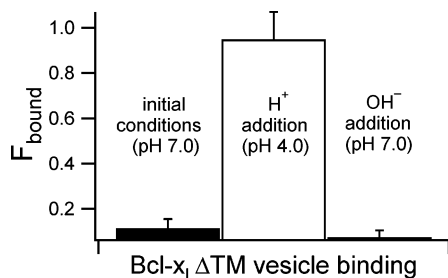


FIGURE 1: Bcl-x_LΔTM associates and dissociates with lipid vesicles as a function of pH. The fraction of protein bound to lipid vesicles (F_{bound}) was measured by a vesicle sedimentation assay, and at pH 7.0, less than 10% of the Bcl-x_LΔTM is membrane-associated. By contrast, when this sample is titrated to pH 4.0 with concentrated HCl, more than 95% of the Bcl-x_LΔTM is membrane-associated. When this sample is titrated back to pH 7.0 with concentrated NaOH, less than 5% of the Bcl-x_LΔTM is membrane-associated, suggesting that Bcl-x_LΔTM reversibly associates with lipid vesicles. The data are means \pm the standard error of the mean of at least three independent measurements using different lipid vesicle and protein preparations.

chemical shifts of a sample of Bcl-x_LΔTM uniformly labeled with ¹⁵N. At pH 7.4 in the absence of lipid vesicles, the NMR chemical shifts are reasonably well-dispersed as expected from a 26.2 kDa molecule with an ~60-residue disordered loop (data not shown). In the presence of anionic lipid vesicles at pH 7.25, this spectrum does not change appreciably as expected (Figure 2a). Upon acidifying this sample to pH 4.65, we noted a disappearance of the majority of cross-peaks in the ¹H–¹⁵N HSQC spectrum (Figure 2b) that presumably was due to association with lipid vesicles with rotational correlation times that are unfavorable for solution NMR spectroscopy. Most likely, the cross-peaks visible in this spectrum arise from unstructured residues not tightly associated with the lipid vesicles. When the pH of this sample was increased to 7.4, we observed a spectrum nearly identical to that of the original sample (Figure 2c). Thus, association of Bcl-x_LΔTM with membranes can be reversed, resulting in a return to its solution conformation.

Bcl-x_LΔTM Increases Monolayer Surface Pressure at pH 5.0 More Than at pH 7.0. To further characterize this membrane association, we measured the changes in the surface pressure of a lipid monolayer upon addition of Bcl-x_LΔTM at pH 7.0 and 5.0 (Figure 3a). In these experiments, the increase in surface pressure upon protein addition is measured, $\Delta\pi$, as a function of the initial surface pressure, π_0 , using a lipid composition similar to that of our previous studies (60:40 DOPC:DOPG). For pH 7.0, at initial surface pressures of 11 mN/m, the surface pressure of the lipid monolayer increases modestly with a change in surface pressure, $\Delta\pi$, of 6 mN/m. As the initial surface pressure is increased, the change in surface pressure upon protein addition decreases as expected. The data fit well to a straight line giving a critical surface pressure, π_c , of 23.6 ± 1.2 mN/m at pH 7.0. By contrast, at pH 5.0 and initial surface pressures above 20 mN/m, we observe a nearly 10-fold increase in the surface pressure with values over 10 mN/m (data not shown). The change in surface pressure upon protein addition also decreases as a function of increasing initial surface pressure. At pH 5.0, the data also are fit well to a straight line, but the critical surface pressure, π_c , increases to 36.9 ± 1.4 mN/m. Thus, addition of Bcl-x_LΔTM at pH 5.0 increases the critical surface pressure of the lipid monolayer

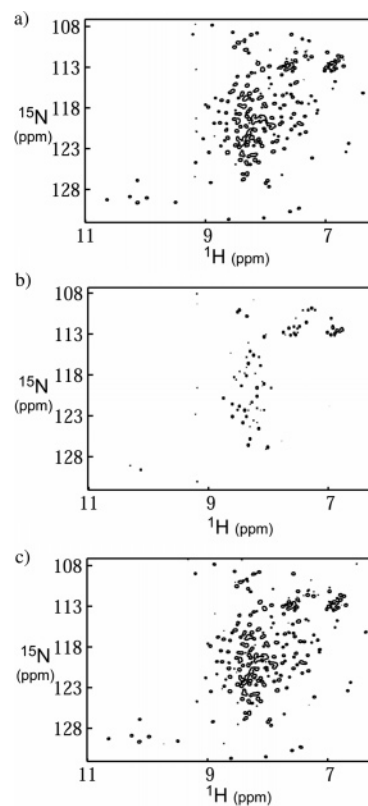


FIGURE 2: Solution conformation of Bcl-x_LΔTM which is unaltered by membrane association as assessed by two-dimensional NMR spectroscopy. (a) ¹⁵N-labeled Bcl-x_LΔTM (60 μM) was incubated overnight with lipid vesicles (60:40 DOPC:DOPG ratio at 25 °C and pH 7.25) at a protein:lipid ratio of 1:200 before a ¹H–¹⁵N HSQC spectrum was recorded at 14.1 T with a cryoprobe. (b) After data collection, the sample was titrated to pH 4.65 by adding small amounts of concentrated HCl and incubated for 10 min before another HSQC spectrum was recorded. Under these conditions, the majority of NMR signals disappear presumably due to the increased rate of transverse relaxation for the protein associated with the lipid vesicle. (c) This sample was then titrated to pH 7.4 by the addition of small amounts of concentrated NaOH and incubated for 10 min. The subsequent HSQC spectrum exhibits the return of the NMR signals with chemical shifts that appear similar to those of the spectrum before acidification.

compared to that at pH 7.0 by 13.3 ± 1.4 mN/m. The critical surface pressure is a measure of the penetration capacity of a protein entering a monolayer: if this pressure exceeds that estimated for a membrane bilayer [32 mN/m (31)], then the protein is thought to be capable of membrane insertion (29–31). Thus, our data are consistent with membrane insertion of Bcl-x_LΔTM at pH 5.0 but not at pH 7.0.

Bcl-x_LΔTM Permeabilizes Lipid Vesicles at pH 5.0 More Than at pH 7.0. To address whether Bcl-x_LΔTM might affect membrane integrity, we assessed the ability of Bcl-x_LΔTM to induce the permeability of lipid vesicles in a dye release assay. In this assay, the fluorescent dye, ANTS, and the collisional quencher, DPX, are encapsulated inside lipid vesicles, resulting in no detectable ANTS fluorescence. When the membrane is compromised, which occurs upon addition of 1% Triton X-100, the subsequent release of ANTS and DPX dilutes the quencher away from the fluorescent dye, resulting in an increase in ANTS fluorescence. Upon addition of Bcl-x_LΔTM at pH 7.0, little change in ANTS fluorescence is detected (Figure 3b). By contrast, upon addition of Bcl-x_LΔTM at pH 5.0, the ANTS fluorescence rapidly increases

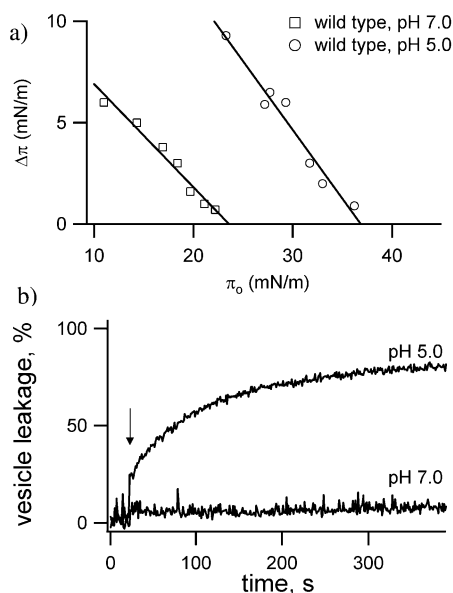


FIGURE 3: Bcl-x_LΔTM increases the surface pressure of lipid monolayers and permeabilizes lipid vesicles in a pH-dependent manner. (a) Changes in surface pressure ($\Delta\pi$) of lipid monolayers (60:40 DOPC:DOPG) after addition of Bcl-x_LΔTM to the subphase are measured as function of the initial surface pressure (π_0) at pH 7.0 (\square) and 5.0 (\circ). The data are fit to a straight line, and the x -intercepts correspond to the monolayer critical surface pressure (π_c), which provides a measure of the membrane penetrability of the protein (29–31). For pH 7.0, the value of π_c is 23.6 ± 1.2 mN/m, which increases to 36.9 ± 1.4 mN/m at pH 5.0. The uncertainty reflects the 95% confidence intervals in π_c from a nonlinear regression analysis of the data. (b) The ability of Bcl-x_LΔTM to cause membrane permeability was assessed at pH 7.0 and 5.0 by a dye leakage assay using ANTS and DPX encapsulated into lipid vesicles (12.5 and 45 mM, respectively, with a final lipid concentration of 0.1 mM) at 37 °C. At pH 7.0, little leakage of ANTS was detected after addition of Bcl-x_LΔTM (denoted with an arrow). At pH 5.0, more than 60% of the ANTS was released after Bcl-x_LΔTM addition. The kinetic traces are representative of at least three independent measurements using two different lipid vesicle preparations. The percentage of leakage was calculated after the complete release of the fluorescent probe by the addition of Triton X-100 [final concentration of 0.1% (w/v)].

and within 7 min is approximately 60% of the signal observed upon addition of detergent. Thus, Bcl-x_LΔTM releases the encapsulated fluorescent dye ANTS from lipid vesicles at pH 5.0, but not at pH 7.0.

Membrane Association of Bcl-x_LΔTM Involves Cooperative Proton Binding. As described above, association of Bcl-x_LΔTM with membranes has been previously demonstrated under conditions that either favor membrane association (typically pH 4.5–5.0) or do not (typically pH 7.4). To determine the nature of this pH dependence, we measured the level of association of Bcl-x_LΔTM with anionic lipid vesicles as a function of pH using the sedimentation assay (Figure 4a). The association of Bcl-x_LΔTM with lipid vesicles is marginal at pH 7.4 but becomes fully associated at lower pH as expected. The nature of the protein binding curve suggests a cooperative pH dependence to association with lipid vesicles. Given that the pK_a value of DOPC and DOPG in large unilamellar vesicles is estimated to be less than 4.0 (32), we attribute the pH dependence to protonation of Bcl-x_LΔTM. We therefore tested whether the vesicle binding data could fit to a simplified thermodynamic linkage model that couples the protonation equilibrium of ionizable residues on the protein surface, pK_a^{app} , with the equilibrium

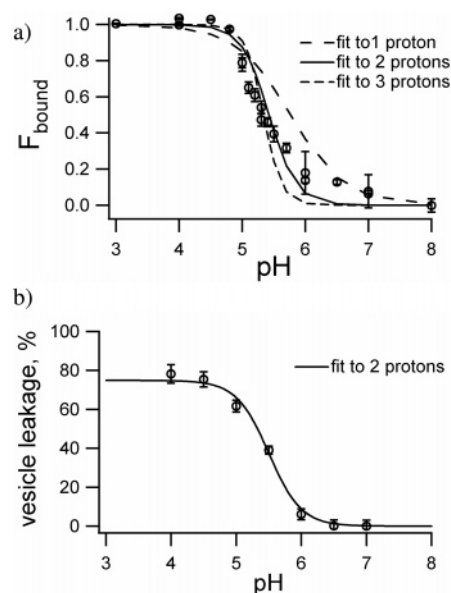


FIGURE 4: Cooperative pH dependence of the solution to membrane conformational change for Bcl-x_LΔTM. (a) The level of association of protein with lipid vesicles (60:40 DOPC:DOPG) was measured as a function of pH by a sedimentation assay. The data are fit to a simplified thermodynamic linkage model that couples protonation to the conformational change. This simplified model assumes protein binds lipid vesicles only upon protonation by any number of protons, n_H , that are governed by a single apparent pK_a^{app} value. From the fits to the data, the number of protons bound to protein (n_H) for the conformational change was estimated to be ~ 2 (—). For comparison, the fits to the data for an n_H of 1 (---) and an n_H of 3 (---) are shown. The values for K_x and pK_a^{app} are interdependent and therefore cannot be determined accurately (see the text). (b) Cooperative pH dependence of Bcl-x_LΔTM-induced leakage of lipid vesicles. The extent of leakage of the fluorescence dye ANTS from lipid vesicles (60:40 DOPC:DOPG) as a function of pH was measured as in Figure 4. The data are reasonably well fit to a similar linkage model with two protons (—).

of binding to the membrane, K_x . In this reductionist model, we make the simplifying assumption that Bcl-x_LΔTM residues protonated during the conformational change can be treated as a single ionizable group governed by a single apparent ionization constant, pK_a^{app} , involving any number of protons, n_H (eqs 2–9). While this is clearly an oversimplification, a nonlinear least-squares fit of the data to this model resulted in reasonable fits with the following parameters: $n_H = 2.1 \pm 0.1$, $pK_a^{app} = 3.5 \pm 0.6$, and $K_x = (2.0 \pm 0.5) \times 10^8$ (uncertainties are 95% confidence limits).

As values and uncertainties derived from multivariable fits can be misleading, we performed a sensitivity analysis to assess their accuracy. Because the slope of the binding curve is directly related to the number of protons, n_H , involved in membrane association, we first estimated the sensitivity of the data to this variable by fitting the data with n_H fixed at 1 or 3 protons. As expected, the data are quite sensitive to this variable, and we conclude that the binding of approximately two protons effects membrane association (Figure 4a). Furthermore, these binding data have been reproduced several times using different preparations of protein and lipid vesicles. In contrast, the values for the apparent ionization constant (pK_a^{app}) and the equilibrium constant for membrane association (K_x) cannot be determined with a high degree of accuracy without further information as they are interdependent.

To confirm the pH dependence of membrane association, we assessed the release of ANTS from lipid vesicles upon addition of Bcl-x_LΔTM as a function of pH. Similar to binding of Bcl-x_LΔTM to lipid vesicles, the level of dye release is marginal at pH 7.4 but increases at lower pH (Figure 4b). Strikingly, these dye release data display a cooperativity similar to that of the vesicle binding data with a slope similar to that of the pH dependence. Indeed, these data are also reasonably well-described by a similar simplified linkage model involving approximately the same number of protons [$n_H = 1.7 \pm 0.7$ (95% confidence interval)]. Therefore, we conclude that protonation of Bcl-x_LΔTM involving approximately two protons is responsible for membrane association and permeabilization.

Two Acidic Residues in the Conserved Hairpin and the Conformational Change. Protonation of Bcl-x_LΔTM affecting membrane association is reminiscent of α-helical bacterial toxins, many of which also undergo a solution-to-membrane conformational change in a pH-dependent manner. These proteins share a similar helical bundle architecture composed of a hydrophobic, helical hairpin surrounded by a sheath of amphiphilic α-helices. Structurally, Bcl-x_LΔTM is most similar to the translocation domain of diphtheria toxin (23). For this toxin, as well as others, membrane association is mediated in part by the so-called hydrophobic, helical hairpin, which corresponds to α-helices 5 and 6 in Bcl-x_LΔTM (Figure 5a) (38–46). Despite the structural similarity, the sequences of these proteins are less than 19% identical, and they possibly are an example of convergent evolution toward a versatile protein fold. However, a curious feature shared by some Bcl-2 proteins and toxins is the presence of acidic residues near the tip of the hairpin (Figure 5b). These acidic residues are curious because many of these proteins are selective for acidic membranes and the hairpin is thought to mediate membrane association (at least for the toxins). Interestingly, for the diphtheria toxin translocation domain, two of the acidic residues (Glu349 or Asp352) have been shown to have altered membrane association and insertion properties (38, 47). Taken together, these observations raise the possibility that acidic residues in this conserved structural feature of Bcl-x_L may become protonated to help mediate membrane association of these proteins with acidic membranes.

One way to evaluate this idea is to test the pH dependence of the conformational change in a mutant of Bcl-x_LΔTM in which conserved acidic residues are replaced with Gln and Asn. We chose to first study a double mutant of Bcl-x_LΔTM, E153Q/D156N, because these two positions correspond to the acidic residues (Glu349 or Asp352) found to be important for the conformational change of the translocation domain from diphtheria toxin (38, 47). Therefore, we characterized Bcl-x_LΔTM-E153Q/D156N for differences in the solution-to-membrane conformational change as measured by vesicle sedimentation, vesicle leakage, and monolayer surface pressure assays.

We first determined that Bcl-x_LΔTM-E153Q/D156N was as well folded as the wild type by circular dichroism spectropolarimetry (data not shown) and then measured its pH dependence of membrane association using the vesicle sedimentation assay. In parallel, we repeated these experiments with the wild-type protein (Figure 6a). At each pH that was measured, the mutant binds better than the wild-

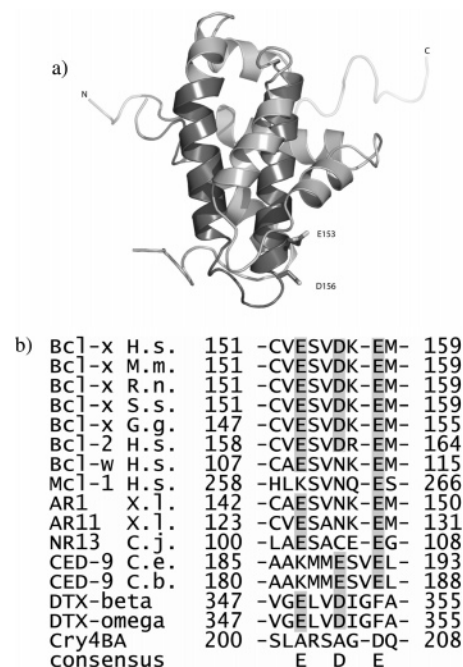


FIGURE 5: Conserved, hydrophobic helical hairpin of Bcl-x_LΔTM that shares acidic residues with bacterial toxins and other Bcl-2 proteins. (a) The so-called hydrophobic, helical hairpin of Bcl-x_LΔTM (α-helices 5 and 6 in darker gray) is postulated to mediate membrane association on the basis of considerations from the bacterial toxins. Residues E153 and D156 in the hairpin are highlighted using a stick representation. The protein is depicted without a large unstructured loop between residues D29 and R77, which is present in the protein used in our experiments. This figure was created using PYMOL (68). (b) Sequence analysis of Bcl-2 proteins and bacterial toxins features acidic residues in the tip of the hairpin between hydrophobic α-helices.

type protein, except below pH 5 where both proteins are fully associated with lipid vesicles. Notably, the difference in membrane binding between the mutant and wild type is approximately the same at each pH above pH 5.0 ($16 \pm 3\%$) (Figure 6b). This observation suggests that the pH dependence of membrane association is similar for both the mutant and wild type and involves approximately the same number of protons. In fact, when we fit the mutant data with a similar model that accounts for 16% of the protein bound at each pH, we obtain an n_H value of ~ 2 , similar to that of the wild type (fit not shown).

An increase in the level of binding of the mutant protein to lipid vesicles might be expected to result in an increase in the extent of membrane permeabilization. Therefore, we measured the ability of E153Q/D156N to cause membrane permeabilization as assessed by the leakage of the fluorescence dye ANTS from lipid vesicles as a function of pH (Figure 6c). In contrast to that of the wild type, the pH dependence of vesicle leakage is shallower for the mutant with an apparent loss of cooperativity. At pH 7.0, both proteins release ANTS from lipid vesicles to the same extent. However, at pH 4.5 where both proteins bind fully, the mutant releases 20% less ANTS (Figure 6d). Thus, for E153Q/D156N, membrane association does not necessarily result in membrane permeability.

Changes in membrane association and permeabilization between the wild type and mutant protein should also be reflected in the critical surface pressures of lipid monolayers. In this measurement, we found that the E153Q/D156N

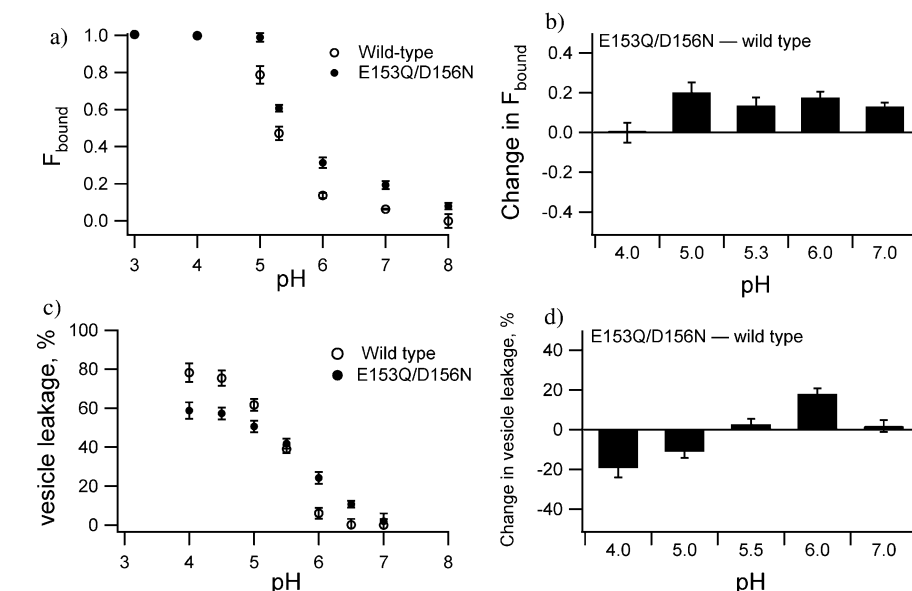


FIGURE 6: E153Q/D156N mutant which differs from wild-type Bcl-x_LΔTM in its pH dependence of membrane association and permeabilization. (a) Binding of protein to lipid vesicles as a function of pH was repeated for Bcl-x_LΔTM (○) concurrently with measurements for E153Q/D156N (●) using the vesicle sedimentation assay as described in the legend of Figure 4a. (b) The difference between the binding of the mutant and wild type to lipid vesicles is shown for pH 4.0–7.0. At each pH that was measured, E153Q/D156N associated as well or better than wild-type Bcl-x_LΔTM. This increase is roughly uniform at each pH between 5.0 and 7.0 ($16 \pm 3\%$). (c) The ability of the E153Q/D156N mutant to induce membrane permeabilization and its pH dependence was also tested. The extent of leakage of the fluorescence dye ANTS from lipid vesicles (60:40 DOPC:DOPG) as a function of pH was measured as described in the legend of Figure 4b. (d) The difference between the mutant and wild type inducing the release of ANTS from lipid vesicles is shown for pH 4.0–7.0. Above pH 5.5, E153Q/D156N induces more ANTS release from lipid vesicles than the wild type. However, below pH 5.5, E153Q/D156N induces less ANTS release from lipid vesicles than the wild type. Each datum is the mean \pm the standard error of the mean of at least three independent measurements using two different lipid vesicle preparations.

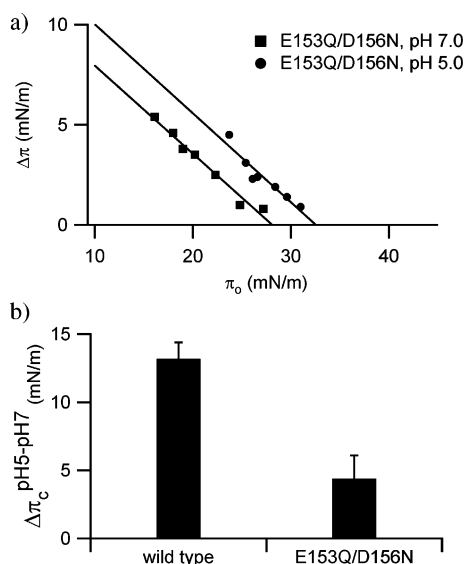


FIGURE 7: E153Q/D156N mutant which differs from wild-type Bcl-x_LΔTM in the pH-dependent changes in monolayer surface pressure. (a) Changes in surface pressure ($\Delta\pi$) of a lipid monolayer at pH 7.0 and 5.0 for E153Q/D156N were measured as described in the legend of Figure 3. At pH 7.0, critical surface pressure π_c increased to 28.1 ± 1.2 mN/m for the mutant, while at pH 5.0, this value decreased to 32.5 ± 1.4 mN/m. (b) These differences are reflected in the pH-dependent change in the critical surface pressure for the lipid monolayer between pH 5.0 and 7.0 ($\Delta\pi_c^{\text{pH5-pH7}}$), which decreases for the E153Q/D156N mutant by 3-fold compared to that of wild-type Bcl-x_LΔTM. The error bars reflect the 95% confidence intervals in π_c from a nonlinear regression analysis of the data.

mutant alters monolayer surface pressure in a manner different from that of the wild-type protein (Figure 7a). At both pH 7.0 and 5.0, addition of the mutant protein gives

rise to the expected linear dependence between the initial surface pressure and the resulting pressure change upon protein addition. However, at pH 7.0, the critical surface pressure increased by 4.5 mN/m to 28.1 ± 1.2 mN/m for the mutant relative to the wild-type protein (Figures 3a and 7a). In contrast, at pH 5.0, the critical surface pressure decreased by 4.4 mN/m to 32.5 ± 1.4 mN/m for the mutant relative to the wild-type protein (Figures 3a and 7a). These pH-dependent differences between the mutant and wild-type protein can be observed via examination of the difference in the critical surface pressure between pH 5.0 and 7.0, $\Delta\pi_c^{\text{pH5-pH7}}$ (Figure 7b). For wild-type Bcl-x_LΔTM, this difference is 13.3 ± 1.4 mN/m, whereas this difference is ~ 3 times smaller for the E153Q/D156N mutant ($\Delta\pi_c^{\text{pH5-pH7}} = 4.4 \pm 1.4$ mN/m).

DISCUSSION

Our results demonstrate reversible association between the N-terminal domain of Bcl-x_L and membranes and suggest this domain is able to insert into and out of the membrane when anchored by its C-terminal transmembrane domain. Using a construct lacking the transmembrane domain was essential for determining what drives membrane association of the N-terminal domain since full-length protein associates with lipid vesicles under conditions where Bcl-x_LΔTM does not (19). The critical surface pressure (π_c) of Bcl-x_LΔTM is consistent with membrane insertion at pH 5.0, but not at pH 7.0 (Figure 3a). This conclusion is further supported by membrane permeabilization of Bcl-x_LΔTM at pH 5.0, but not at pH 7.0 (Figure 3b). While membrane permeabilization can arise from many types of protein–membrane interactions, our results are consistent with a model for the

membrane conformation in which some elements of Bcl-x_L span the bilayer. Multiple lines of evidence lend support to this model, including the ion conductance properties of Bcl-x_LΔTM, which presumably would require spanning the bilayer (15, 16, 19, 21, 22, 48). Thus, it appears that the N-terminal domain of Bcl-x_L can be tightly associated with the membrane, even span the bilayer, and do so reversibly. Such reversibility, while surprising, has been also demonstrated for the translocation domain of diphtheria toxin that is structurally similar with Bcl-x_L and the C helix of bacteriorhodopsin (49–51).

These data allow us to refine our model for the conformational change of full-length Bcl-x_L that involves at least three distinct conformations, one solution and two membrane (19). In this model, the solution conformation is similar to the known structure of Bcl-x_LΔTM (23), with the exception that the C-terminal transmembrane domain is tucked into its own BH3 binding pocket as in the structure of Bax, a pro-apoptotic Bcl-2 family member (52). One membrane conformation is proposed to be “tail-inserted” with the structure of the N-terminal domain similar to the solution conformation, but anchored at the membrane surface by the C-terminal transmembrane domain. In this conformation, access to the BH3 binding pocket of Bcl-x_L is no longer occluded by its TM and it is now freely open and poised to bind ligands. The other membrane conformation involves membrane association of the N-terminal domain and from the data presented here suggests significant protein–bilayer interactions occur in this conformation. Notably, our data also suggest reversibility of membrane insertion for the N-terminal domain of Bcl-x_L. Whether such reversibility is a general feature of Bcl-2 family members is not known but might be a general way in which these proteins are regulated. Consistent with this idea, membrane insertion of the N-terminal domain of another pro-survival family member, Bcl-2, appears to be necessary to prevent Bax activation (13). Perhaps Bcl-x_L uses a similar mechanism to prevent Bak and Bax activation.

Membrane Association Arises from Weakening Electrostatic Repulsion. Membrane association occurs upon protonation of Bcl-x_LΔTM, which could either strengthen the electrostatic attraction or weaken the electrostatic repulsion with the negatively charged surface of the membrane. Because this pH effect occurs between pH 7 and 5, protonation of histidine residues (pK_a value typically ~6.5) may be important in this process, as demonstrated for the pH-dependent membrane association of peptides (53). However, Bcl-x_LΔTM is an acidic protein with an estimated pI of ~4.4 that would be expected to elevate histidine pK_a values. Indeed, we have measured the pK_a values of its four histidines by long-range HMQC in the absence of membranes and found that these values are ~7.0 (data not shown). These values would expect to be further elevated in the presence of the negatively charged membranes used here. Therefore, association with a negatively charged membrane most likely does not arise from an increase in the level of electrostatic attraction upon protonation and likely arises from a decrease in the level of electrostatic repulsion that occurs upon protonation of acidic residues with pK_a values elevated from the canonical values of ~4.0.

Our results with a mutant of Bcl-x_LΔTM also lend support to this idea. Mutating two conserved acidic residues, E153

and D156, resulted in a small, but reproducible, increase in the level of membrane association with negatively charged lipid vesicles. Because the increase in the level of membrane association was approximately the same at each pH (~20%), the slope of the pH dependence is approximately the same for the mutant ($n_H \sim 2$; fit not shown) and the wild-type protein. Therefore, these data suggest that the E153Q and D156N mutations act by weakening the electrostatic repulsion between the mutant protein and negatively charged membrane and are not involved in the cooperative pH dependence.

By contrast, these two residues do affect the cooperative pH dependence of membrane leakage by Bcl-x_LΔTM, which is significantly less cooperative for the mutant than for the wild-type protein (Figure 6c,d). Why does an increased level of membrane binding not result in an increased level of membrane leakage? One possibility is that membrane leakage is a two-step process requiring both membrane binding that is favored by the mutant and membrane insertion that is not. The critical surface pressure of the mutant protein is consistent with this possibility since this value decreased at pH 5.0 to below the “membrane penetrability” value (Figures 3a and 7). A decreased level of membrane insertion may arise from the unfavorable free energy of transfer from water to the membrane for Gln/Asn residues compared to protonated Glu/Asp residues (54–56). Thus, our data are consistent with a model in which acidic residues in a conserved hairpin, E153 and D156, are important to both membrane binding and insertion but contribute significantly only to the proton cooperativity of membrane insertion and not to binding. Interestingly, acidic residues in similar positions of the conserved helical hairpin of the translocation domain from diphtheria toxin are important for membrane insertion (38, 44, 47, 57–59).

Perhaps protonation of acidic residues is involved in the reversibility of proteins that insert into membranes. In addition to Bcl-x_L, the translocation domain of diphtheria toxin also reversibly inserts into membranes in a pH-dependent manner. Furthermore, protonation of acidic residues is involved in the reversibility of membrane spanning for the C helix of bacteriorhodopsin, in which two of its six acidic residues are embedded in the bilayer (49). We speculate here that acidic residues are responsible for the observed reversibility because of the innate differences in the membrane partitioning properties of protonated and ionized Glu and Asp, which could readily be exploited as a reversibility switch. Protonated Glu and Asp residues are more favorable than the ionized species by ~1.5–2 kcal/mol per residue (water/octanol) in model peptide studies (54–56). Thus, protonating acidic residues might favor membrane association, whereas deprotonating these residues would favor disassociation and possibly account for the observed reversibility. Such a mechanism may be universal as other proteins are known to reversibly associate with membranes upon protonation (60, 61). These proteins are part of a larger class of proteins that reversibly associate with membranes called amphitropic proteins (62). In this sense, Bcl-x_L can be thought to possess an amphitropic N-terminal domain because of its ability to reversibly associate with membranes.

Protonation of Bcl-x_L by two protons to effect membrane insertion does not mean that only two acidic residues are

being protonated. Bcl-x_L contains 31 Glu and Asp residues evenly distributed throughout the structure and suggests a tightly coupled electrostatic network involving many acidic residues. For Bcl-x_LΔTM when we remove two acidic residues, the midpoint of the pH transition changes significantly, but little change is seen in the slope of this transition. These results seem consistent with an ensemble of conformational substates in which many of the acidic residues participate in protonation and this conformational change. In this scenario, small changes in the microscopic substates can result in much larger macroscopic changes because of shifts in the substate populations. In our case, perhaps the E153Q/D156N mutant causes such a shift in the ensemble of conformational substates in a manner similar to that recently proposed to drive the pH-dependent unfolding of staphylococcal nuclease (63, 64).

In summary, the N-terminal domain of Bcl-x_L, in the absence of its transmembrane domain, reversibly inserts into the membrane upon binding approximately two protons. In the context of the full-length protein, we speculate that fewer protons will be necessary for membrane insertion, resulting in a reversible conformational change at physiologically relevant pH values. This prediction is based upon the full-length protein already being attached to the membrane surface, and it is therefore likely that the proton binding required for this initial attraction in the absence of the transmembrane domain may not be necessary. Cytosolic pH is thought to change significantly during apoptosis (11, 65–67). Therefore, reversibility of the Bcl-x_L membrane insertion by a pH-dependent mechanism might be important for the regulation of apoptosis in vivo (11).

ACKNOWLEDGMENT

We are grateful to Bertrand García-Moreno, Joel R. Tolman, Diana Murray, and Kevin R. MacKenzie for many helpful discussions. We also thank Frederick J. Tan and Lora K. Picton for reading of the manuscript.

REFERENCES

- Chao, D. T., and Korsmeyer, S. J. (1998) BCL-2 Family: Regulators of Cell Death, *Annu. Rev. Immunol.* 16, 395–419.
- Gross, A. (2001) BCL-2 Proteins: Regulators of the Mitochondrial Apoptotic Program, *IUBMB Life* 52, 231–6.
- Harris, M. H., and Thompson, C. B. (2000) The Role of the Bcl-2 Family in the Regulation of Outer Mitochondrial Membrane Permeability, *Cell Death Differ.* 7, 1182–91.
- Kuwana, T., and Newmeyer, D. D. (2003) Bcl-2-Family Proteins and the Role of Mitochondria in Apoptosis, *Curr. Opin. Cell Biol.* 15, 691–9.
- Schendel, S. L., Montal, M., and Reed, J. C. (1998) Bcl-2 Family Proteins as Ion Channels, *Cell Death Differ.* 5, 372–80.
- Sharpe, J. C., Arnoult, D., and Youle, R. J. (2004) Control of Mitochondrial Permeability by Bcl-2 Family Members, *Biochim. Biophys. Acta* 1644, 107–13.
- Shimizu, S., Narita, M., and Tsujimoto, Y. (1999) Bcl-2 Family Proteins Regulate the Release of Apoptogenic Cytochrome c by the Mitochondrial Channel VDAC, *Nature* 399, 483–7.
- Fannjiang, Y., Cheng, W. C., Lee, S. J., Qi, B., Pevsner, J., McCaffery, J. M., Hill, R. B., Basanez, G., and Hardwick, J. M. (2004) Mitochondrial Fission Proteins Regulate Programmed Cell Death in Yeast, *Genes Dev.* 18, 2785–97.
- Youle, R. J., and Karbowski, M. (2005) Mitochondrial Fission in Apoptosis, *Nat. Rev. Mol. Cell Biol.* 6, 657–63.
- Wolter, K. G., Hsu, Y. T., Smith, C. L., Nechushtan, A., Xi, X. G., and Youle, R. J. (1997) Movement of Bax from the Cytosol to Mitochondria during Apoptosis, *J. Cell Biol.* 139, 1281–92.
- Hsu, Y. T., Wolter, K. G., and Youle, R. J. (1997) Cytosol-to-Membrane Redistribution of Bax and Bcl-X(L) during Apoptosis, *Proc. Natl. Acad. Sci. U.S.A.* 94, 3668–72.
- Kuwana, T., Mackey, M. R., Perkins, G., Ellisman, M. H., Latterich, M., Schneider, R., Green, D. R., and Newmeyer, D. D. (2002) Bid, Bax, and Lipids Cooperate to Form Supramolecular Openings in the Outer Mitochondrial Membrane, *Cell* 111, 331–42.
- Dlugosz, P. J., Billen, L. P., Annis, M. G., Zhu, W., Zhang, Z., Lin, J., Leber, B., and Andrews, D. W. (2006) Bcl-2 Changes Conformation to Inhibit Bax Oligomerization, *EMBO J.* 25, 2287–96.
- Yang, E., Zha, J., Jockel, J., Boise, L. H., Thompson, C. B., and Korsmeyer, S. J. (1995) Bad, a Heterodimeric Partner for Bcl-XL and Bcl-2, Displaces Bax and Promotes Cell Death, *Cell* 80, 285–91.
- Minn, A. J., Kettlun, C. S., Liang, H., Kelekar, A., Vander Heiden, M. G., Chang, B. S., Fesik, S. W., Fill, M., and Thompson, C. B. (1999) Bcl-xL Regulates Apoptosis by Heterodimerization-Dependent and -Independent Mechanisms, *EMBO J.* 18, 632–43.
- Minn, A. J., Velez, P., Schendel, S. L., Liang, H., Muchmore, S. W., Fesik, S. W., Fill, M., and Thompson, C. B. (1997) Bcl-x(L) Forms an Ion Channel in Synthetic Lipid Membranes, *Nature* 385, 353–7.
- Vander Heiden, M. G., Li, X. X., Gottlieb, E., Hill, R. B., Thompson, C. B., and Colombini, M. (2001) Bcl-xL Promotes the Open Configuration of the Voltage-Dependent Anion Channel and Metabolite Passage through the Outer Mitochondrial Membrane, *J. Biol. Chem.* 276, 19414–9.
- Basanez, G., Zhang, J., Chau, B. N., Maksaev, G. I., Frolov, V. A., Brandt, T. A., Burch, J., Hardwick, J. M., and Zimmerberg, J. (2001) Pro-Apoptotic Cleavage Products of Bcl-xL Form Cytochrome c-Conducting Pores in Pure Lipid Membranes, *J. Biol. Chem.* 276, 31083–91.
- Thuduppathy, G. R., Craig, J. W., Kholodenko, V., Schon, A., and Hill, R. B. (2006) Evidence that Membrane Insertion of the Cytosolic Domain of Bcl-x(L) is Governed by an Electrostatic Mechanism, *J. Mol. Biol.* 359, 1045–58.
- Thuduppathy, G. R., and Hill, R. B. (2006) Acid Destabilization of the Solution Conformation of Bcl-xL does Not Drive its pH-Dependent Insertion into Membranes, *Protein Sci.* 15, 248–57.
- Losonczi, J. A., Olejniczak, E. T., Betz, S. F., Harlan, J. E., Mack, J., and Fesik, S. W. (2000) NMR Studies of the Anti-Apoptotic Protein Bcl-xL in Micelles, *Biochemistry* 39, 11024–33.
- Franzin, C. M., Choi, J., Zhai, D., Reed, J. C., and Marassi, F. M. (2004) Structural Studies of Apoptosis and Ion Transport Regulatory Proteins in Membranes, *Magn. Reson. Chem.* 42, 172–9.
- Muchmore, S. W., Sattler, M., Liang, H., Meadows, R. P., Harlan, J. E., Yoon, H. S., Nettlesheim, D., Chang, B. S., Thompson, C. B., Wong, S. L., Ng, S. L., and Fesik, S. W. (1996) X-Ray and NMR Structure of Human Bcl-xL, an Inhibitor of Programmed Cell Death, *Nature* 381, 335–41.
- Sambrook, J., and Russell, D. W. (2001) *Molecular Cloning: A Laboratory Manual*, 3rd ed., Cold Spring Harbor Laboratory Press, Plainview, NY.
- Wimley, W. C., Hristova, K., Ladokhin, A. S., Silvestro, L., Axelsen, P. H., and White, S. H. (1998) Folding of β -Sheet Membrane Proteins: A Hydrophobic Hexapeptide Model, *J. Mol. Biol.* 277, 1091–110.
- MacDonald, R. C., MacDonald, R. I., Menco, B. P., Takeshita, K., Subbarao, N. K., and Hu, L. R. (1991) Small-Volume Extrusion Apparatus for Preparation of Large, Unilamellar Vesicles, *Biochim. Biophys. Acta* 1061, 297–303.
- Perrin, D. D. (1963) Buffers of Low Ionic Strength for Spectrophotometric pK Determinations, *Aust. J. Chem.* 16, 572–8.
- Bradford, M. M. (1976) A Rapid and Sensitive Method for the Quantitation of Microgram Quantities of Protein Utilizing the Principle of Protein-Dye Binding, *Anal. Biochem.* 72, 248–54.
- Colacicco, G. (1970) Lipid Monolayers: Mechanisms of Protein Penetration with Regard to Membrane Models, *Lipids* 5, 636–49.
- Verger, R., and Pattus, F. (1982) Lipid-Protein Interactions in Monolayers, *Chem. Phys. Lipids* 30, 189–227.
- Kimelberg, H. K., and Papahadjopoulos, D. (1971) Phospholipid-Protein Interactions: Membrane Permeability Correlated with Monolayer “Penetration”, *Biochim. Biophys. Acta* 233, 805–9.
- Cevc, G., and Marsh, D. (1987) *Phospholipid Bilayers: Physical Principles and Models*, John Wiley & Sons, New York.

33. Bartlett, G. R. (1959) Phosphorus Assay in Column Chromatography, *J. Biol. Chem.* 234, 466–8.
34. Ellens, H., Bentz, J., and Szoka, F. C. (1985) H^+ - and Ca^{2+} -Induced Fusion and Destabilization of Liposomes, *Biochemistry* 24, 3099–106.
35. Delaglio, F., Grzesiek, S., Vuister, G. W., Zhu, G., Pfeifer, J., and Bax, A. (1995) NMRPipe: A Multidimensional Spectral Processing System Based on UNIX Pipes, *J. Biomol. NMR* 6, 277–93.
36. Johnson, B. A., and Blevins, R. A. (1994) NMRView: A Computer Program for the Visualization and Analysis of NMR Data, *J. Biomol. NMR* 4, 603–14.
37. Johnson, B. A. (2004) Using NMRView to Visualize and Analyze the NMR Spectra of Macromolecules, *Methods Mol. Biol.* 278, 313–52.
38. Silverman, J. A., Mindell, J. A., Finkelstein, A., Shen, W. H., and Collier, R. J. (1994) Mutational Analysis of the Helical Hairpin Region of Diphtheria Toxin Transmembrane Domain, *J. Biol. Chem.* 269, 22524–32.
39. Zakharov, S. D., and Cramer, W. A. (2002) Colicin Crystal Structures: Pathways and Mechanisms for Colicin Insertion into Membranes, *Biochim. Biophys. Acta* 1565, 333–46.
40. Li, J., Derbyshire, D. J., Promdonkoy, B., and Ellar, D. J. (2001) Structural Implications for the Transformation of the *Bacillus thuringiensis* Delta-Endotoxins from Water-Soluble to Membrane-Inserted Forms, *Biochem. Soc. Trans.* 29, 571–7.
41. Lambotte, S., Jasperse, P., and Bechinger, B. (1998) Orientational Distribution of α -Helices in the Colicin B and E1 Channel Domains: A One and Two Dimensional ^{15}N Solid-State NMR Investigation in Uniaxially Aligned Phospholipid Bilayers, *Biochemistry* 37, 16–22.
42. Lakey, J. H., Massotte, D., Heitz, F., Dasseux, J. L., Faucon, J. F., Parker, M. W., and Pattus, F. (1991) Membrane Insertion of the Pore-Forming Domain of Colicin A. A Spectroscopic Study, *Eur. J. Biochem.* 196, 599–607.
43. Malenbaum, S. E., Collier, R. J., and London, E. (1998) Membrane Topography of the T Domain of Diphtheria Toxin Probed with Single Tryptophan Mutants, *Biochemistry* 37, 17915–22.
44. Kachel, K., Ren, J., Collier, R. J., and London, E. (1998) Identifying Transmembrane States and Defining the Membrane Insertion Boundaries of Hydrophobic Helices in Membrane-Inserted Diphtheria Toxin T Domain, *J. Biol. Chem.* 273, 22950–6.
45. Lakey, J. H., Duche, D., Gonzalez-Manas, J. M., Baty, D., and Pattus, F. (1993) Fluorescence Energy Transfer Distance Measurements. The Hydrophobic Helical Hairpin of Colicin A in the Membrane Bound State, *J. Mol. Biol.* 230, 1055–67.
46. Parker, M. W., and Pattus, F. (1993) Rendering a Membrane Protein Soluble in Water: A Common Packing Motif in Bacterial Protein Toxins, *Trends Biochem. Sci.* 18, 391–5.
47. Kaul, P., Silverman, J., Shen, W. H., Blanke, S. R., Huynh, P. D., Finkelstein, A., and Collier, R. J. (1996) Roles of Glu 349 and Asp 352 in Membrane Insertion and Translocation by Diphtheria Toxin, *Protein Sci.* 5, 687–92.
48. Garcia-Saez, A. J., Mingarro, I., Perez-Paya, E., and Salgado, J. (2004) Membrane-Insertion Fragments of Bcl-xL, Bax, and Bid, *Biochemistry* 43, 10930–43.
49. Hunt, J. F., Rath, P., Rothschild, K. J., and Engelman, D. M. (1997) Spontaneous, pH-Dependent Membrane Insertion of a Transbilayer α -Helix, *Biochemistry* 36, 15177–92.
50. Senzel, L., Gordon, M., Blaustein, R. O., Oh, K. J., Collier, R. J., and Finkelstein, A. (2000) Topography of Diphtheria Toxin's T Domain in the Open Channel State, *J. Gen. Physiol.* 115, 421–34.
51. Ladokhin, A. S., Legmann, R., Collier, R. J., and White, S. H. (2004) Reversible Refolding of the Diphtheria Toxin T-Domain on Lipid Membranes, *Biochemistry* 43, 7451–8.
52. Suzuki, M., Youle, R. J., and Tjandra, N. (2000) Structure of Bax: Coregulation of Dimer Formation and Intracellular Localization, *Cell* 103, 645–54.
53. Bechinger, B. (1996) Towards Membrane Protein Design: pH-Sensitive Topology of Histidine-Containing Polypeptides, *J. Mol. Biol.* 263, 768–75.
54. White, S. H., and Wimley, W. C. (1999) Membrane Protein Folding and Stability: Physical Principles, *Annu. Rev. Biophys. Biomol. Struct.* 28, 319–65.
55. Wimley, W. C., Creamer, T. P., and White, S. H. (1996) Solvation Energies of Amino Acid Side Chains and Backbone in a Family of Host-Guest Pentapeptides, *Biochemistry* 35, 109–24.
56. Wimley, W. C., and White, S. H. (1996) Experimentally Determined Hydrophobicity Scale for Proteins at Membrane Interfaces, *Nat. Struct. Biol.* 3, 842–8.
57. Zhan, H., Elliott, J. L., Shen, W. H., Huynh, P. D., Finkelstein, A., and Collier, R. J. (1999) Effects of Mutations in Proline 345 on Insertion of Diphtheria Toxin into Model Membranes, *J. Membr. Biol.* 167, 173–81.
58. Zhan, H., Choe, S., Huynh, P. D., Finkelstein, A., Eisenberg, D., and Collier, R. J. (1994) Dynamic Transitions of the Transmembrane Domain of Diphtheria Toxin: Disulfide Trapping and Fluorescence Proximity Studies, *Biochemistry* 33, 11254–63.
59. O'Keefe, D. O., Cabiaux, V., Choe, S., Eisenberg, D., and Collier, R. J. (1992) pH-Dependent Insertion of Proteins into Membranes: B-Chain Mutation of Diphtheria Toxin that Inhibits Membrane Translocation, Glu-349 \rightarrow Lys, *Proc. Natl. Acad. Sci. U.S.A.* 89, 6202–6.
60. Johnson, J. E., Xie, M., Singh, L. M., Edge, R., and Cornell, R. B. (2003) Both Acidic and Basic Amino Acids in an Amphitropic Enzyme, CTP:Phosphocholine Cytidylyltransferase, Dictate its Selectivity for Anionic Membranes, *J. Biol. Chem.* 278, 514–22.
61. Chenal, A., Vernier, G., Savarin, P., Bushmarina, N. A., Geze, A., Guillain, F., Gillet, D., and Forge, V. (2005) Conformational States and Thermodynamics of α -Lactalbumin Bound to Membranes: A Case Study of the Effects of pH, Calcium, Lipid Membrane Curvature and Charge, *J. Mol. Biol.* 349, 890–905.
62. Johnson, J. E., and Cornell, R. B. (1999) Amphitropic Proteins: Regulation by Reversible Membrane Interactions, *Mol. Membr. Biol.* 16, 217–35.
63. Fitch, C. A., Whitten, S. T., Hilser, V. J., and Garcia-Moreno, E. B. (2006) Molecular Mechanisms of pH-Driven Conformational Transitions of Proteins: Insights from Continuum Electrostatics Calculations of Acid Unfolding, *Proteins* (in press).
64. Whitten, S. T., Garcia-Moreno, E. B., and Hilser, V. J. (2005) Local Conformational Fluctuations can Modulate the Coupling between Proton Binding and Global Structural Transitions in Proteins, *Proc. Natl. Acad. Sci. U.S.A.* 102, 4282–7.
65. Lagadic-Gossman, D., Huc, L., and Lecureur, V. (2004) Alterations of Intracellular pH Homeostasis in Apoptosis: Origins and Roles, *Cell Death Differ.* 11, 953–61.
66. Matsuyama, S., Llopis, J., Deveraux, Q. L., Tsien, R. Y., and Reed, J. C. (2000) Changes in Intramitochondrial and Cytosolic pH: Early Events that Modulate Caspase Activation during Apoptosis, *Nat. Cell Biol.* 2, 318–25.
67. Matsuyama, S., and Reed, J. C. (2000) Mitochondria-Dependent Apoptosis and Cellular pH Regulation, *Cell Death Differ.* 7, 1155–65.
68. DeLano, W. L. (2002) *PyMOL Molecular Graphics System*, DeLano Scientific, San Carlos, CA.

BI0616652